



Published in final edited form as:

Mucosal Immunol. 2018 September ; 11(5): 1398–1407. doi:10.1038/s41385-018-0037-0.

T cell-directed IL-17 production by lung granular $\gamma\delta$ T cells is coordinated by a novel IL-2 and IL-1 β circuit

Antoine Ménoret^{1,2}, James A. Buturla³, Maria M. Xu¹, Julia Svedova¹, Sanjeev Kumar¹, Vijay A. K. Rathinam¹, Anthony T. Vella¹

¹Department of Immunology, UConn Health, 263 Farmington Avenue, Farmington, CT 06030, USA; ²Institute for Systems Genomics, UConn Health, 400 Farmington Avenue, Farmington, CT 06030, USA and ³Department of Internal Medicine, UConn Health, 263 Farmington Avenue, Farmington, CT 06030, USA

Abstract

Immune-mediated lung is considered the result of an exacerbated innate injury immune response, although a role for adaptive lymphocytes is emerging. $\alpha\beta$ T cells specific for *S. aureus* enterotoxin A orchestrate a T $\gamma\delta$ 17 response during lung injury. However, the mechanism driving IL-17 production is unclear. Here, we show a role for IL-2 triggering IL-17 production by lung granular $\gamma\delta$ T cells as IL-17 synthesis and neutrophil recruitment was reduced by IL-2 blocking mAbs in vitro and in vivo. Mass cytometry analysis revealed that lung $\gamma\delta$ T cells responded directly to IL-2 as evident from STAT5 phosphorylation and RoR γ t expression. IL-2 receptor blocking mAbs and JAK inhibition impaired STAT5 phosphorylation and IL-17 release. Moreover, inhalation of *S. aureus* enterotoxin A induced IL-2 secretion and caspase-1-dependent IL-1 β activation to drive IL-17 production. This T-cell-mediated inflammasome-dependent IL-17 response is maximum when lung T $\gamma\delta$ 17 cells were sequentially stimulated first with IL-2 then IL-1 β . Interestingly, when IL-2 is given therapeutically to cancer patients it carries a known risk of lung injury that is largely indistinguishable from that seen in sepsis. Hence, this novel mechanism reveals therapeutic targets treating both acute lung injury and high-dose IL-2 toxicity in cancer.

INTRODUCTION

Recent evidence shows that T cells can regulate innate immunity,¹ such as memory T cells facilitating innate immune cell recruitment amplifying local immunity.^{2–4} Although acute lung injury and acute respiratory distress syndrome (ALI/ARDS) have been considered to be driven by the innate immune response, evidence for the participation of T cells is emerging. Consistent with a role for T cells in ALI/ARDS, several reports observed a significant

Correspondence: Antoine Ménoret (menoret@uchc.edu) or Anthony T. Vella (vella@uchc.edu). A.T.V. and A.M. conceived and designed the study. A.T.V., A.M., and J.A.B. analyzed the data. A.T.V. and A.M. drafted the manuscript. A.M., M.M.X., J.S., J.A.B., and S.K. performed experiments. J.A.B. provided computational expertise, developed the CyTOF analysis protocol. J.A.B. and M.M.X. reviewed the manuscript. V.A.R. provided reagents, experimental expertise and reviewed the manuscript.

ADDITIONAL INFORMATION

The online version of this article (<https://doi.org/10.1038/s41385-018-0037-0>) contains supplementary material, which is available to authorized users.

increase in CD4 and CD8 T cells expressing activation and proliferation markers in bronchoalveolar lavage (BAL) of patients during the early phase of ARDS.^{5,6} Moreover, specific $\alpha\beta$ T cells drive lung injury in mice after inhalation of *Staphylococcus aureus* enterotoxin.⁷⁻⁹

Importantly, interleukin (IL)-2 is regarded as a biomarker for ARDS severity.^{10,11} When IL-2 is given therapeutically to cancer patients it carries a known risk of lung injury that is largely indistinguishable from that seen in sepsis.^{12,13} Similarly, IL-2 administration to rats induces pulmonary inflammation.^{14,15} Altogether these observations suggest a role for T cells and IL-2 in ALI/ARDS.

Staphylococcus aureus infection contributes to higher morbidity/mortality during influenza coinfection¹⁶ and healthcare-associated pneumonia,¹⁷ and is a major cause of ARDS associated with pneumonia.^{18,19} Host defense against *S. aureus* lung infection has been shown to be mediated by $\gamma\delta$ T cells.²⁰ This might be related to the role of $\gamma\delta$ T cells as a primary source of IL-17, which facilitates bacterial clearance, but also contributes to lung injury during *S. aureus* lung infection. A major virulence mechanism of *S. aureus* is the release of enterotoxins that are well known to induce lethal toxic shock in people.^{21,22} These enterotoxins are regarded as superantigens since, without being processed, they bind MHC II and link specific V β regions of the TCR on T cells to drive massive production of cytokines and proliferation.²³⁻²⁵ We recently demonstrated that after *S. aureus* enterotoxin A inhalation, lung $\gamma\delta$ T cells produced IL-17, even though they are not known to bind *S. aureus* enterotoxin A, but interestingly they required $\alpha\beta$ T cells for their activation.²⁶

Here, we describe how $\alpha\beta$ T cells induce pulmonary $\gamma\delta$ T-cell activation. The data demonstrate that enterotoxins induce rapid release of IL-2, which activates pulmonary $\gamma\delta$ T cells to synthesize pro-inflammatory IL-17. Ex vivo culture of pulmonary $\gamma\delta$ T cells with IL-2 -induced IL-17 production and CyTOF analysis demonstrated STAT5 activation and RoR γ t expression within a small subpopulation of granular T $\gamma\delta$ 17 cells. This contrasts from the antagonizing role IL-2 plays in Th17 differentiation,²⁷ and shows that IL-17 release from T $\gamma\delta$ 17 cells is JAK/STAT dependent. Mechanistically, we found that IL-2 worked in concert with IL-1 β to drive IL-17 production by both bulk and sorted lung $\gamma\delta$ T cells. Thus, our data suggests that high levels of IL-2 activates T $\gamma\delta$ 17 cells, producing IL-17 driven pulmonary injury. Moreover, IL-2 cancer immunotherapy could be void of adverse IL-17-based events with the use of IL-17 blockade.

MATERIALS AND METHODS

Mice

C57BL/6 and caspase 1/11^{-/-} (stock #16621) mice were purchased from the Jackson Laboratory (Bar Harbor, ME). Caspase 11^{-/-} mice were the kind gift of Vishva Dixit (Genentech) and Kate Fitzgerald (University of Massachusetts Medical School). All mice were maintained in the central animal facility at the University of Connecticut Health (UCH) in accordance with federal guidelines. The present study was approved by the UCH's Animal Care Committee.

Reagents

Staphylococcus enterotoxin A (*S. aureus* enterotoxin A) was purchased from Toxin Technology Inc. (Sarasota, FL). Mouse recombinant IL-1 β was purchased from Life Technologies (Carlsbad, CA). Human rIL-2 was obtained from the NIH. Ionomycin was purchased from Life Technology (Grand Island, NY). Phorbol 12-Myristate 13-Acetate (PMA) and Brefeldin A (BFA) were purchased from EMD Millipore Corporation (Billerica, MA). Ruxolitinib (sc-364729) was purchased from Santa Cruz Biotechnology (Santa Cruz, CA). Heparin was purchased from Thermo Fisher Scientific (Waltham, MA). Collagenase (from *Clostridium histolyticum* IV), Lipopolysaccharide (LPS) (from salmonella enterica typhimurium), MgCl₂, and CaCl₂ were purchased from Sigma Aldrich (St. Louis, MO). Live/Dead UV blue stain was purchased from Invitrogen (San Diego, CA).

Antibodies and enzyme-linked immunosorbent assay (ELISA) Anti-IL-1 β (clone B122) and anti-CD122 (clone TM- β 1) were purchased from Biolegend (San Diego, CA). Anti-IL-2 antibodies (clones S4B6-1 and JES6-1A12), anti-CD25 antibody (clone PC-61.5.3) and rat isotype controls were purchased from Bio X Cell (West Lebanon, NH). Anti-IL-23 antibody (#AF1619) was purchased from R&D Systems (Minneapolis, MN). IL-1 β , IL-2, and tumor necrosis factor (TNF) ELISA kits were purchased from BD Bioscience (San Jose, CA). IL-17 and IL-23 ELISA kits were purchased from eBioscience (San Diego, CA). Anti-CD4-V450, -CD3-AF700, -IL-17-Percp Cy5.5, -CD4 biot (clone GK1.5), -NK1.1 (clone PK136) were purchased from BD biosciences (San Jose, CA). Anti-TCR δ -PE-Cy7 (clone GL3), -MHC class II (I/A-E), -PECAM1/CD31 (clone 390) were purchased from eBioscience. Anti-TCR δ 1.1-FITC (clone 2.11), Anti-TCR δ 2-PE (clone UC3-10A6), Anti-TCR δ 3-APC (clone 536) were purchased from Biolegend (San Diego, CA). Anti-CD8 biot was purchased from Leinco Technologies, Inc (St Louis, MO). All metal-conjugated antibodies, barcoding kit Cell-ID 20-plex (#201060), viability stain Cell-ID Cisplatin (#201064), DNA intercalator Cell-ID intercalator-Ir 125 μ M (#201192 A), CyTOF buffers Maxpar Perm-S buffer (#201066) Maxpar Fix I buffer (#201065), Maxpar Fix & Perm buffer (#201067), Maxpar water (#201069) and Maxpar cell staining buffer (#201068) were purchased from Fluidigm (South San Francisco, CA).

Tissue processing and cell isolation

BAL was collected by lavage of mouse lung with sterile PBS. BAL was centrifuged at 1000 rpm at 4 °C to separate cells from BALF and 0.2 μ m filtered as described earlier.²⁸ Lungs were homogenized post-BAL lavage using MagNA Lyser Green Beads (Roche, Basel, Switzerland) at 6000 rpm. Protein was quantified using BCA assay (Thermo Fisher Scientific, Waltham, MA). Lymph node cells obtained from axillary and inguinal lymph nodes were crushed through 100 μ m nylon mesh cell strainers (BD Biosciences), washed with BSS and counted using ZI particle counter (Beckman Coulter). Lung cells were obtained as described before.²⁶ Briefly, lung tissue was perfused with PBS-heparin (0.055 g/L), cut into small pieces, and incubated with 1.3 mM EDTA/PBS at 37 °C for 20 min, washed, followed by digestion with collagenase solution containing collagenase from *Clostridium histolyticum* IV (150 U/ml), 1 mM MgCl₂, 1 mM CaCl₂, in BSS, at 37 °C for 20 min. Subsequently digested lung tissues were crushed through 100 μ m nylon mesh cell strainers (BD Biosciences) and partitioned between a 44 and 67% Percoll gradient to obtain

cells at the interface. For CyTOF experiments, lung cells were processed with a few modifications to facilitate the flow of cells through the CyTOF. Briefly, lung tissue was perfused with PBS/EDTA, washed and digested at 37 °C for 30 min with collagenase solution containing DNase I (60 Unit/ml). Residual lung tissue was crushed through 40 µm nylon mesh cell strainers (BD Biosciences) and cells were purified using Lympholyte M (Cedarlane Labs, Burlington, NC). $\gamma\delta$ T cell were enriched by negative magnetic isolation with Dynabeads biotin binder (Invitrogen) and biotinylated antibodies to CD8 (2.43), CD4 (GK1.5), MHC class II (I/A-E), PECAM1/CD31 (390) and NK1.1 (PK136). CD3+ GL3+ cells were sorted from the enriched population on a FACS Aria II (BD).

Flow cytometry and CyTOF

Flow cytometry was performed as described before.⁸ Cells processed for CyTOF experiments were labeled with Cell-ID™ Cisplatin to identify live and dead cells and subsequently barcoded with Cell-ID™ Pd Barcoding kit (all CyTOF reagents are from Fluidigm, San Francisco, CA). Barcoded samples were pooled together, fixed with Maxpar Fix I buffer, permeabilized with methanol, incubated with FcR blocking solution and 25 heavy metal-conjugated antibodies. DNA was labeled using Cell-ID™ Intercalator-Ir. The pooled sample was spiked with normalization beads and analyzed by a mass cytometer (Helios, Fluidigm). The data were debarcoded using the Fluidigm Debarcoder v1.04. A single-cell gate and a live cell gate were obtained from each sample. The samples were further sub-gated to include the same number of cells per sample and merged to create the viSNE maps (MATLAB; MathWorks, Natick, MA) using only the non-signaling markers. Histograms comparing the expression of signaling and activation markers were generated using MATLAB,²⁹ similar to our previous approach.³⁰

Immunization and cytokine neutralization

Mice were anesthetized with isoflurane (Vedco Inc., Saint Joseph, MO) and given 1 or 0.25 µg of *S. aureus* enterotoxin A (as indicated in figure legend) diluted in 50 µl of BSS, or BSS alone by intranasal (i.n.) route as previously described.²⁶ IL-2 neutralization was carried out by intraperitoneal injection of 1 mg of anti-IL-2 antibody clone S4B6 and 1 mg of anti-IL-2 antibody clone JES6-1A12 30 min prior to *S. aureus* enterotoxin A immunization. Rat IgG was used as a control in a separate group. In vitro antibody neutralization was carried out using antibodies specific for IL-1 β (clone B122), IL-2 (clones S4B6-1 and JES6-1A12), IL-23 (clone AF1619), CD25 (clone PC-61.5.3), CD122 (clone TM- β 1).

In vitro and ex vivo cell culture

Cells were cultured for 20 h, or the indicated time, at 37 °C and 5% CO₂ in 200 µl complete tumor medium (CTM), consisting of modified Eagle's medium with 5% fetal bovine serum, amino acids, salts and antibiotics. Cells were seeded in 96-well round-bottom plates and stimulated with media alone, *S. aureus* enterotoxin A (0.5 µg/ml), rmIL1 β (10 ng/ml), rhIL-2 (100U/ml), or PMA (50 ng/ml; Calbiochem, Darmstadt, Germany) plus ionomycin (1 µg/ml; Invitrogen). For analysis of secreted cytokines, tissue culture plates were centrifuged and tissue culture medium analyzed by ELISA. For intracellular cytokine staining analysis, BFA was added to the culture and cells were stimulated as indicated in figure legend. Cells were stained and analyzed by flow cytometry.

Statistical analysis

A two-tailed Student's unpaired test was used for data analysis, with values of $p < 0.05$ (*) used as significant threshold; $p < 0.01$ is indicated as (**) and $p < 0.001$ as (***). All statistical analyses were performed using Prism-GraphPad (La Jolla, CA).

RESULTS

$\gamma\delta$ T cells respond to *S. aureus* enterotoxin A by producing IL-17 through an IL-2-dependent cytokine circuit

Lung $\gamma\delta$ T cells release IL-17 within hours of *S. aureus* enterotoxin A inhalation, but a strict requirement for the presence of TCR $\alpha\beta$ T cells during this process is noted.²⁶ To uncover the role each tissue-specific T-cell population plays, *S. aureus* enterotoxin A-driven IL-17 synthesis was explored in an in vitro co-culture assay involving lung cells (as source of lung $\gamma\delta$ T cells), and lymph node (LN) cells (as source of $\alpha\beta$ T cells). After an overnight culture $\gamma\delta$ T cells producing IL-17A (herein referred to as IL-17) were detected, but only those with increased Side Scatter (SSC) scale (termed hereafter as lung granular $\gamma\delta$ T cells) were capable of synthesizing IL-17 (Fig. 1a, b). No other population of IL-17⁺ producer was detected (Supplementary Fig. 1a) and the TCR usage of these granular IL-17⁺ $\gamma\delta$ T cells was mainly TCR V γ 2⁺ (V γ 1⁻2⁻3⁻) with a slightly greater percentage TCR V γ 2⁺ as compared to IL-17⁻ cells (Supplementary Fig. 2). Finally, IL-17 detection by intracellular cytokine staining required the absence of brefeldin A (BFA) in the first 6 h (Fig. 1a), as continual BFA presence in the culture resulted in no IL-17 production (Supplementary Fig. 1b), suggesting a secreted factor such as a cytokine after *S. aureus* enterotoxin A stimulation was required for IL-17 synthesis by the granular $\gamma\delta$ T cells.

Cytokines secreted into the culture were measured and, consistent with the intracellular cytokine staining in Fig. 1a, IL-17 was detected at high levels when LN and lung cells were co-cultured (Fig. 1c, top panel). Perhaps surprisingly, the Th17 expansion cytokine IL-23³¹ was not detected above background (Fig. 1c, middle), but IL-2 was significantly produced by LN cells cultured alone or with lung cells (Fig. 1c, bottom). We postulated that IL-2 might induce IL-17 production by lung granular $\gamma\delta$ T cells.

This was tested by incubating LN+ lung cells with *S. aureus* enterotoxin A and anti-IL-2 mAb to inhibit IL-2 function. The results demonstrated a significant reduction in IL-17 during IL-2 neutralization (Fig. 1d). Additionally, lung cells stimulated in vitro with IL-2 produced IL-17 by granular $\gamma\delta$ T cells, but only modestly when stimulated with other cytokines such as IL-3, IL-4, IL-7, IL-15, IL-17, IFN γ , and TGF β (Supplementary Fig. 3). Ultimately, this contrasts with the prevailing idea that IL-2 suppresses Th17 cell differentiation.²⁷ One possibility to explain this apparent contradiction, is that the granular $\gamma\delta$ T cells, characterized by the expression of the key Th17 transcription factor RoR γ t, may be fully differentiated to IL-17 expression under conducive conditions in the lung.

Defining lung granular $\gamma\delta$ T cells as differentiated T $\gamma\delta$ 17 cells Granular $\gamma\delta$ T cells in the lung constitute a rare population, Mass cytometry (CyTOF) was utilized to characterize this population. CyTOF analysis revealed $\gamma\delta$ T cells as positive for CD3 and TCR $\gamma\delta$, and

negative for many other markers such as CD4, CD8, MHC II, Gr-1, CD11b, CD11c, CD19, NK1.1, Siglec-F (Fig. 2). As shown in Fig. 2a, after viSNE mapping, granular $\gamma\delta$ T cells segregated into discrete subpopulations that either express high or very low levels of RoR γ t. Most importantly the RoR γ t^{hi} cells (herein referred to as T $\gamma\delta$ 17 cells) were concurrently positive for pSTAT5 4 h after *S. aureus* enterotoxin A inhalation (Fig. 2a, b). Other non-T $\gamma\delta$ 17 cells express high RoR γ t but were negative for pSTAT5, pSTAT1, and pSTAT3 (Supplementary Fig. 4a). pSTAT1 and pSTAT3 also were elevated in T $\gamma\delta$ 17 after *S. aureus* enterotoxin A inhalation and pSTAT1 was slightly elevated in RoR γ t^{lo} cells as well (Fig. 2b). Thus, the lung T $\gamma\delta$ 17 cells responded to *S. aureus* enterotoxin A with specific increases in pSTAT5 suggesting that they responded locally in vivo to the cytokine milieu.

Confirming that lung T $\gamma\delta$ 17 cells are directly able to respond to IL-2, STAT5 phosphorylation was observed in lung RoR γ t^{hi}, but not in RoR γ t^{low}, T $\gamma\delta$ 17 cells from naive mice upon stimulation with IL-2 (Supplementary Fig. 4b). Moreover, when blocking mAbs specific for either the high-affinity (CD25) or low-affinity (CD122) IL-2 receptors were added to an in vitro culture prior to IL-2 stimulation, a modest decrease in pSTAT5 expression was observed, but robust inhibition occurred upon neutralization of both IL-2 receptors (Fig. 3a, b). Similarly, the non-granular lung $\gamma\delta$ T cells also expressed pSTAT5 after IL-2 exposure suggesting that their lack of IL-17 production (Fig. 1) was a consequence of very low RoR γ t. To further test the pathway responsible for IL-17 synthesis, IL-2R signaling was blocked using Ruxolitinib, a JAK inhibitor known to interfere with phosphorylation of STAT5.³² IL-17 production by lung cells stimulated with IL-2 was significantly inhibited with Ruxolitinib (Fig. 3c), but importantly TNF synthesis by the same cells stimulated with PMA+ ionomycin was not affected (Fig. 3d). Thus, IL-2 promotes IL-17 release by lung T $\gamma\delta$ 17 cells.

Lung T $\gamma\delta$ 17 cells rely on IL-2 and inflammasomes activated by *S. aureus* enterotoxin A

Since the data uncovered the presence of pSTAT5⁺ lung T $\gamma\delta$ 17 cells (Fig. 3), an early event in IL-2 signaling, it was reasoned that IL-2 release occurred rapidly after *S. aureus* enterotoxin A inhalation. Over a 48 h time period IL-2 levels in serum, lung tissue, and BAL fluid were measured by ELISA (Fig. 4a). IL-17 was also detected in BAL fluid 24 h post *S. aureus* enterotoxin A inhalation (Supplementary Fig. 5). Importantly, a fast and robust release of IL-2 was evident at 4 h in all tissues examined followed by a rapid decline (Fig. 4a). While these data demonstrate the presence of circulating IL-2 and its localized presence in lung, they do not show that IL-2 actually impacts the lung T $\gamma\delta$ 17 cells in vivo after *S. aureus* enterotoxin A inhalation.

To test this idea a strategy was used to neutralize IL-2 in vivo, which as noted by others can be difficult to achieve.³³ A previously documented method using anti-IL-2 mAbs with specificity to IL-2 and to the IL-2 receptor was employed.³⁴ Immunization with 1 μ g of enterotoxin released high local and systemic IL-2 levels (Fig. 4a) that were difficult to neutralize. However, a low dose of enterotoxin (0.25 μ g) still induced substantial IL-17 expression by the lung T $\gamma\delta$ 17 cells, which was significantly inhibited by IL-2 blockade (Fig. 4b,c). Neutrophil accumulation in the lung was also inhibited by IL-2 blockade (Fig. 4d). Supported by previous results demonstrating that lung T $\gamma\delta$ 17 cells depend on TCR $\alpha\beta$ T

cells to produce IL-17,²⁶ and that gut effector memory Th17 cells are induced by systemic enterotoxin administration,³⁵ it was postulated that IL-2 plays a role in IL-17 synthesis. However, IL-2 does not likely function alone in this capacity.

Several cytokines direct Th17 differentiation including IL-1 β , IL-6, TGF β , and IL-23. Of these we found no evidence for IL-23's involvement (Fig. 1c) even after IL-2 stimulation (Supplementary Fig. 6a), which suggested that IL-1 β might be the best candidate since it is necessary for optimal gut $\gamma\delta$ T-cell IL-17 responses.³⁶ This was tested in mice intranasally (i.n.) treated for 6 h with vehicle, *S. aureus* enterotoxin A, or bacterial LPS (to serve as an innate immune driver of IL-17). After cell isolation and 5 h culture the vehicle alone resulted in background IL-17 synthesis but the immunized mice yielded lung T $\gamma\delta$ 17 cells with robust IL-17 production (Fig. 5a). In the *S. aureus* enterotoxin A-treated mice, ex vivo IL-1 β neutralization substantially inhibited IL-17 production, but interestingly IL-1 β neutralization had no effect in the LPS-treated mice (Fig. 5a, b). These data suggest that *S. aureus* enterotoxin A inhalation promotes IL-2 release that, along with IL-1 β , drives lung T $\gamma\delta$ 17 cell IL-17 production. To test this mechanism, we evaluated if lung $\gamma\delta$ T cells were readily capable to respond to IL-2 and IL-1 β . Lung cells from naive mice were stimulated with IL-2 in the presence of IL-1 β neutralization (Fig. 5c) or with CD25 blockade (Fig. 5d). IL-2 with blockade of IL-1 β or CD25 resulted in significantly reduced IL-17 production (Fig. 5c, d), and IL-23 blockade had no effect (Supplementary Fig. 6a). Moreover, IL-2 blockade did not affect IL-23-induced IL-17 (Supplementary Fig. 6b).

To define this mechanism further, and test if IL-1 β is matured by inflammasome activated caspase 1, caspase 1/11^{-/-} mice were treated with vehicle or *S. aureus* enterotoxin A for 6 h and then lung cells were cultured ex vivo followed by intracellular IL-17 measurement. The data show markedly less production of IL-17 in caspase 1/11^{-/-} cells (Fig. 6a, b), which suggests that caspases 1 and/or 11 play a role in promoting the maturation of IL-1 β that, in combination with IL-2, induces IL-17 synthesis. Secondly, offering IL-2 to wild-type or caspase 11^{-/-} cells induced IL-17 release, but caspase 1/11^{-/-} cells produced significantly less IL-17 (Fig. 6c). Specifically, IL-17 production in wild-type and caspase 11^{-/-} cells was inhibited when IL-1 β was neutralized, and adding IL-1 β with IL-2 rescued IL-17 release in caspase 1/11^{-/-} cells, whereas IL-1 β alone did not. Finally, the sequence of cytokine addition for optimal IL-17 release was determined using caspase 1/11^{-/-} lung cells to control for the IL-1 β level in culture. Neither IL-2 nor IL-1 β alone promoted IL-17 production (Fig. 6d, first three columns), and IL-17 production was greatest with IL-2 stimulation before IL-1 β (Fig. 6d, last two columns). Similarly, in sorted wild-type lung $\gamma\delta$ T cells, neither IL-2 nor IL-1 β alone promoted IL-17 production, but they synergized to produce IL-17 when given together (Fig. 6e).

DISCUSSION

A growing body of research shows that T cells function as antigen-specific sentinels that alert the local innate cells to respond to infection and tissue damage.^{2, 3, 37} We have previously shown that *S. aureus* enterotoxin A-specific $\alpha\beta$ T cells regulate IL-17 synthesis by lung $\gamma\delta$ T cells, affecting neutrophil recruitment, but the molecular mechanism was unclear.²⁶ Here, we show that IL-2 release in synergy with caspase-1 dependent IL-1 β production is required

for IL-17 production by lung T $\gamma\delta$ 17 cells. These data demonstrate that IL-2 from $\alpha\beta$ T cells can compromise pulmonary homeostasis, dependent on an IL-1 β checkpoint.

Our study provides evidence that granular T $\gamma\delta$ 17 cells are the only source of IL-17 in response to pulmonary *S. aureus* enterotoxin A challenge (Fig. 1a and Supplementary Fig. 1a). This cell population differed from classical $\gamma\delta$ T cells by its higher granularity and expression of granzyme B (Fig. 1a and data not shown). However, TCR specificity did not seem a key factor as IL-17-producing granular lung T $\gamma\delta$ 17 cells expressed similar TCR γ chain than non-producing cells (Supplementary Fig. 2). In this model, IL-17 production was inhibited by IL-2 blockade in vitro (Fig. 1d), and in vivo (Fig. 4d, c) and IL-2 itself induced IL-17 production by granular lung T $\gamma\delta$ 17 cells (Fig. 3c, Supplementary Figs. 3 and 6 and Supplementary Fig. 6). From a mechanistic perspective, we observed that shortly after *S. aureus* enterotoxin A inhalation RoR γ t-expressing $\gamma\delta$ T cells phosphorylated STAT5 and STAT3 (Fig. 2). A similar CyTOF approach demonstrated that RoR γ t⁺ T $\gamma\delta$ 17 cells from steady-state lung are capable of responding directly to IL-2 by rapidly phosphorylating STAT5 (Supplementary Fig. 4b). The detection of pSTAT5 and pSTAT3 in lung T $\gamma\delta$ 17 cells suggests that both transcription factors contribute to IL-17 production as observed in other systems.³⁸ Moreover, our data suggest that T $\gamma\delta$ 17 cells from naive lung used the IL-2 signaling pathway to phosphorylate STAT5 and express IL-17 (Fig. 3). From a translational perspective, the inhibition of IL-17 synthesis mediated by Ruxolitinib (a FDA approved JAK1 and JAK2 inhibitor^{39, 40}) offers new avenues for ALI/ARDS intervention. The low but constitutive level of pSTAT5 detected in lung T $\gamma\delta$ 17 cells in the absence of exogenous stimulation suggests that this subpopulation of cells has the potential to rapidly respond to cytokines in steady-state lung and initiate local inflammation. These data demonstrated a key role for IL-2 in facilitating IL-17 production, contrasting from the established inhibitory role of IL-2 on Th17 polarization.^{27, 38} Hence, IL-2 promotes rapid IL-17 synthesis by lung T $\gamma\delta$ 17 cells to initiate innate immunity at the site of insult or damage and neutrophil recruitment (Fig. 4d), while inhibiting Th17 differentiation and systemic IL-17-mediated inflammation. Mapping STAT5 binding in lung T $\gamma\delta$ 17 by ChIPseq and deleting the relevant sites by CRISP/Cas9 technology would provide new insight in the epigenetic regulation of IL-17.

Our model revealed that T cells stimulated IL-1 β activation which is required for granular lung T $\gamma\delta$ 17 cell IL-17 production in synergy with IL-2 (Figs. 5 and 6). We demonstrated the requirement for IL-1 β ex vivo using neutralizing anti-IL-1 β (Fig. 5a,b), and in vivo using caspase 1/11^{-/-} mice challenged intranasally with *S. aureus* enterotoxin A (Fig. 6a, b). This observation is surprising but consistent with the inflammasome-dependent production of IL-17 by $\gamma\delta$ T cells previously observed at the site of *S. aureus* infection.⁴¹ It is also possible that some IL-1 β was produced by other mechanisms independent of the inflammasome but not tested in this study.⁴² Additional studies will be required to find the cellular source of IL-1 β , but it is perhaps not by coincidence that $\gamma\delta$ T cells throughout the lung of naive mice have been found predominantly in physical contact with MHC II⁺ and F4/80⁺ myeloid cells that could function to release IL-1 β .⁴³ Moreover, MHC II is expressed by alveolar macrophages and dendritic cells,⁴⁴ and *S. aureus* enterotoxin A inhalation induces rapid migration of monocytes to lung and upregulation of MHC II.^{7, 26} In contrast with other studies showing that CD11c⁺ cells produced a large quantity of IL-23 in

LPS-induced lung injury,⁴⁵ and CD103⁺ dendritic cells produce IL-23 in response to invasive pulmonary aspergillosis,⁴⁶ our study shows IL-17 production that appears independent of IL-23 (Fig. 1c and Supplementary Fig. 6a, b). The apparent lack of IL-23 and the absence of direct $\gamma\delta$ TCR activation are consistent with a novel mechanism where IL-1 β and IL-2 bind lung T $\gamma\delta$ 17 cells and induce IL-17 production. Directly related to this alternate mechanism is the appearance of maximal IL-17 levels only when lung T $\gamma\delta$ 17 cells are first stimulated with IL-2 then with IL-1 β (Fig. 6d). This was confirmed by using sorted lung $\gamma\delta$ T cells stimulated with IL-2 then with IL-1 β (Fig. 6e). This is strikingly similar to adjuvant function where out-of-sequence adjuvant signals corrupt cellular responses.^{47, 48} Thus, inflammation is tightly regulated not only by the specific cytokine or costimulatory mediators but also by their sequential triggering of receptors.

Our data indicated that local inflammation could be promoted by a subpopulation of lung T $\gamma\delta$ 17 cells in response to a high level of systemic IL-2 and local IL-1 β to produce and release IL-17. Lung $\gamma\delta$ T cells are known to produce IL-17, cause inflammation and initiate lung injury,^{20, 49} but our study precisely defines a subpopulation of lung T $\gamma\delta$ 17 cells that bridges the systemic adaptive immune system with local innate signals. The outcome of this response is lung inflammation, which could explain why cancer treatment with high IL-2 doses induces side effects remarkably similar to pulmonary injury in sepsis.^{12, 13} Hence, targeting lung T $\gamma\delta$ 17 could be an innovative approach to both limit lung inflammation during ALI/ARDS and decrease the toxicity of IL-2-based cancer immunotherapy.

Altogether, our study sheds new light on a novel link between $\alpha\beta$ T cells and lung T $\gamma\delta$ 17 cells, provides a new mechanism contributing to the understanding of the toxicity of high IL-2 levels, and underscores the importance of targeting cytokines in the development of new therapeutic interventions against lung injury.

Supplementary Material

Refer to Web version on PubMed Central for supplementary material.

ACKNOWLEDGEMENTS

We would like to thank Drs. Adam J. Adler and Kepeng Wang (Dept. of Immunology, UConn Health, Farmington, CT) for insightful discussions. This study was supported by NIH/NIAID P01AI056172. S.K. is currently at Department of Life Science and Bioinformatics, Assam University, 788 011 Assam, India.

REFERENCES

1. Gasteiger G Is adaptive-innate lymphocyte cross-talk driving mucosal disease? Proc. Natl Acad. Sci. USA 114, 1220–1222 (2017). [PubMed: 28126720]
2. Schenkel JM, Fraser KA, Vezys V & Masopust D Sensing and alarm function of resident memory CD8(+) T cells. Nat. Immunol 14, 509–513 (2013). [PubMed: 23542740]
3. Gasteiger G & Rudensky AY Interactions between innate and adaptive lymphocytes. Nat. Rev. Immunol 14, 631–639 (2014). [PubMed: 25132095]
4. Ariotti S et al. T cell memory. Skin-resident memory CD8(+) T cells trigger a state of tissue-wide pathogen alert. Science 346, 101–105 (2014). [PubMed: 25278612]

5. Risso K et al. Early infectious acute respiratory distress syndrome is characterized by activation and proliferation of alveolar T-cells. *Eur. J. Clin. Microbiol. Infect. Dis.: Off. Publ. Eur. Soc. Clin. Microbiol* 34, 1111–1118 (2015).
6. Li JT et al. Unexpected role for adaptive alphabetaTh17 cells in acute respiratory distress syndrome. *J. Immunol. (Baltim., Md. : 1950)* 195, 87–95 (2015).
7. Muralimohan G, Rossi RJ, Guemsey LA, Thrall RS & Vella AT Inhalation of *Staphylococcus aureus* enterotoxin A induces IFN-gamma and CD8 T cell-dependent airway and interstitial lung pathology in mice. *J. Immunol. (Baltim., Md. : 1950)* 181, 3698–3705 (2008).
8. Menoret A, Kumar S & Vella AT Cytochrome b5 and cytokeratin 17 are biomarkers in bronchoalveolar fluid signifying onset of acute lung injury. *PLoS ONE* 7, e40184 (2012). [PubMed: 22792238]
9. Neumann B, Engelhardt B, Wagner H & Holzmann B Induction of acute inflammatory lung injury by staphylococcal enterotoxin B. *J. Immunol* 158, 1862–1871 (1997). [PubMed: 9029127]
10. Lesur O et al. Interleukin-2 involvement in early acute respiratory distress syndrome: relationship with polymorphonuclear neutrophil apoptosis and patient survival. *Crit. Care Med* 28, 3814–3822 (2000). [PubMed: 11153619]
11. Terpstra ML, Aman J, van Nieuw Amerongen GP & Groeneveld AB Plasma biomarkers for acute respiratory distress syndrome: a systematic review and meta-analysis*. *Crit. Care Med* 42, 691–700 (2014). [PubMed: 24158164]
12. Gores KM et al. Plasma angiopoietin 2 concentrations are related to impaired lung function and organ failure in a clinical cohort receiving high-dose interleukin 2 therapy. *Shock* 42, 115–120 (2014). [PubMed: 24727870]
13. Dutcher JP Current status of interleukin-2 therapy for metastatic renal cell carcinoma and metastatic melanoma. *Oncol. (Williston Park)* 16, 4–10 (2002).
14. Ishizaka A et al. Prevention of interleukin 2-induced acute lung injury in guinea pigs by pentoxifylline. *J. Appl. Physiol.* (1985) 67, 2432–2437 (1989). [PubMed: 2606851]
15. Abdih H, Kelly CJ, Bouchier-Hayes D, Barry M & Kearns S Taurine prevents interleukin-2-induced acute lung injury in rats. *Eur. Surg. Res* 32, 347–352 (2000). [PubMed: 11182618]
16. Rice TW et al. Critical illness from 2009 pandemic influenza A virus and bacterial coinfection in the United States. *Crit. Care Med* 40, 1487–1498 (2012). [PubMed: 22511131]
17. Kollef MH et al. Epidemiology and outcomes of health-care-associated pneumonia: results from a large US database of culture-positive pneumonia. *Chest* 128, 3854–3862 (2005). [PubMed: 16354854]
18. Xu Y et al. Differential susceptibility of human Sp-B genetic variants on lung injury caused by bacterial pneumonia and the effect of a chemically modified curcumin. *Shock* 45, 375–384 (2016). [PubMed: 26863117]
19. Napolitano LM, Brunsvold ME, Reddy RC & Hyzy RC Community-acquired methicillin-resistant *Staphylococcus aureus* pneumonia and ARDS: 1-year follow-up. *Chest* 136, 1407–1412 (2009). [PubMed: 19892681]
20. Cheng P et al. Role of gamma-delta T cells in host response against *Staphylococcus aureus*-induced pneumonia. *BMC Immunol.* 13, 38 (2012). [PubMed: 22776294]
21. Leung DY et al. Toxic shock syndrome toxin-secreting *Staphylococcus aureus* in Kawasaki syndrome. *Lancet* 342, 1385–1388 (1993). [PubMed: 7901681]
22. Garbe PL et al. *Staphylococcus aureus* isolates from patients with nonmenstrual toxic shock syndrome. *Evid. Addit. toxins. JAMA* 253, 2538–2542 (1985).
23. Marrack P, Blackman M, Kushnir E & Kappler J The toxicity of staphylococcal enterotoxin B in mice is mediated by T cells. *J. Exp. Med* 171, 455–464 (1990). [PubMed: 2303780]
24. Choi YW et al. Residues of the variable region of the T-cell-receptor beta-chain that interact with *S. aureus* toxin superantigens. *Nature* 346, 471–473 (1990). [PubMed: 2377208]
25. Miethke T et al. T cell-mediated lethal shock triggered in mice by the superantigen staphylococcal enterotoxin B: critical role of tumor necrosis factor. *J. Exp. Med* 175, 91–98 (1992). [PubMed: 1730929]
26. Kumar S et al. Rapid alphabeta T-cell responses orchestrate innate immunity in response to Staphylococcal enterotoxin A. *Mucosal Immunol.* 6, 1006–1015 (2013). [PubMed: 23321986]

27. Laurence A et al. Interleukin-2 signaling via STAT5 constrains T helper 17 cell generation. *Immunity* 26, 371–381 (2007). [PubMed: 17363300]
28. Menoret A, Svedova J, Behl B & Vella AT Trace levels of Staphylococcal enterotoxin bioactivity are concealed in a mucosal niche during pulmonary inflammation. *PLoS ONE* 10, e0141548 (2015). [PubMed: 26509442]
29. Amir el AD et al. viSNE enables visualization of high dimensional single-cell data and reveals phenotypic heterogeneity of leukemia. *Nat. Biotechnol* 31, 545–552 (2013). [PubMed: 23685480]
30. Svedova J et al. Therapeutic blockade of CD54 attenuates pulmonary barrier damage in T cell-induced acute lung injury. *Am. J. Physiol. Lung Cell. Mol. Physiol* 313, L177–L191 (2017). [PubMed: 28473322]
31. Bettelli E et al. Reciprocal developmental pathways for the generation of pathogenic effector TH17 and regulatory T cells. *Nature* 441, 235–238 (2006). [PubMed: 16648838]
32. Verstovsek S et al. Safety and efficacy of INCB018424, a JAK1 and JAK2 inhibitor, in myelofibrosis. *N. Engl. J. Med* 363, 1117–1127 (2010). [PubMed: 20843246]
33. Boyman O, Kovar M, Rubinstein MP, Surh CD & Sprent J Selective stimulation of T cell subsets with antibody-cytokine immune complexes. *Science* 311, 1924–1927 (2006). [PubMed: 16484453]
34. Boyman O & Sprent J The role of interleukin-2 during homeostasis and activation of the immune system. *Nat. Rev. Immunol* 12, 180–190 (2012). [PubMed: 22343569]
35. Szabo PA et al. Rapid and rigorous IL-17A production by a distinct subpopulation of effector memory T lymphocytes constitutes a novel mechanism of toxic shock syndrome immunopathology. *J. Immunol* 198, 2805–2818 (2017). [PubMed: 28219889]
36. Duan J, Chung H, Troy E & Kasper DL Microbial colonization drives expansion of IL-1 receptor 1-expressing and IL-17-producing gamma/delta T cells. *Cell Host Microbe* 7, 140–150 (2010). [PubMed: 20159619]
37. Bihl F et al. Primed antigen-specific CD4+ T cells are required for NK cell activation in vivo upon *Leishmania major* infection. *J. Immunol* 185, 2174–2181 (2010). [PubMed: 20624944]
38. Yang XP et al. Opposing regulation of the locus encoding IL-17 through direct, reciprocal actions of STAT3 and STAT5. *Nat. Immunol* 12, 247–254 (2011). [PubMed: 21278738]
39. Beauverd Y, McLornan DP, Radia DH & Harrison CN Ruxolitinib: evolution or revolution in treatment of patients with polycythemia vera? *Future Oncol.* 12, 739–749 (2016). [PubMed: 26846873]
40. Harrison CN, Talpaz M & Mead AJ Ruxolitinib is effective in patients with intermediate-1 risk myelofibrosis: a summary of recent evidence. *Leuk. Lymphoma* 57, 2259–2267 (2016). [PubMed: 27463690]
41. Maher BM et al. Nlrp-3-driven interleukin 17 production by gammadeltaT cells controls infection outcomes during *Staphylococcus aureus* surgical site infection. *Infect. Immun* 81, 4478–4489 (2013). [PubMed: 24082072]
42. Hildebrand D et al. Granzyme A produces bioactive IL-1beta through a non-apoptotic inflammasome-independent pathway. *Cell Rep.* 9, 910–917 (2014). [PubMed: 25437548]
43. Wands JM et al. Distribution and leukocyte contacts of gammadelta T cells in the lung. *J. Leukoc. Biol* 78, 1086–1096 (2005). [PubMed: 16204632]
44. Aggarwal NR, King LS & D'Alessio FR Diverse macrophage populations mediate acute lung inflammation and resolution. *Am. J. Physiol. Lung Cell. Mol. Physiol* 306, L709–L725 (2014). [PubMed: 24508730]
45. Bosmann M et al. CD11c+ alveolar macrophages are a source of IL-23 during lipopolysaccharide-induced acute lung injury. *Shock* 39, 447–452 (2013). [PubMed: 23481504]
46. Zelante T et al. CD103(+) Dendritic cells control Th17 cell function in the lung. *Cell Rep.* 12, 1789–1801 (2015). [PubMed: 26365185]
47. Sckisel GD et al. Out-of-sequence signal 3 paralyzes primary CD4(+) T-cell-dependent immunity. *Immunity* 43, 240–250 (2015). [PubMed: 26231116]
48. Benci JL et al. Tumor interferon signaling regulates a multigenic resistance program to immune checkpoint blockade. *Cell* 167, 1540–1554 e1512 (2016). [PubMed: 27912061]

49. Chien YH, Meyer C & Bonneville M Gammadelta T cells: first line of defense and beyond. *Annu. Rev. Immunol* 32, 121–155 (2014). [PubMed: 24387714]

Author Manuscript

Author Manuscript

Author Manuscript

Author Manuscript

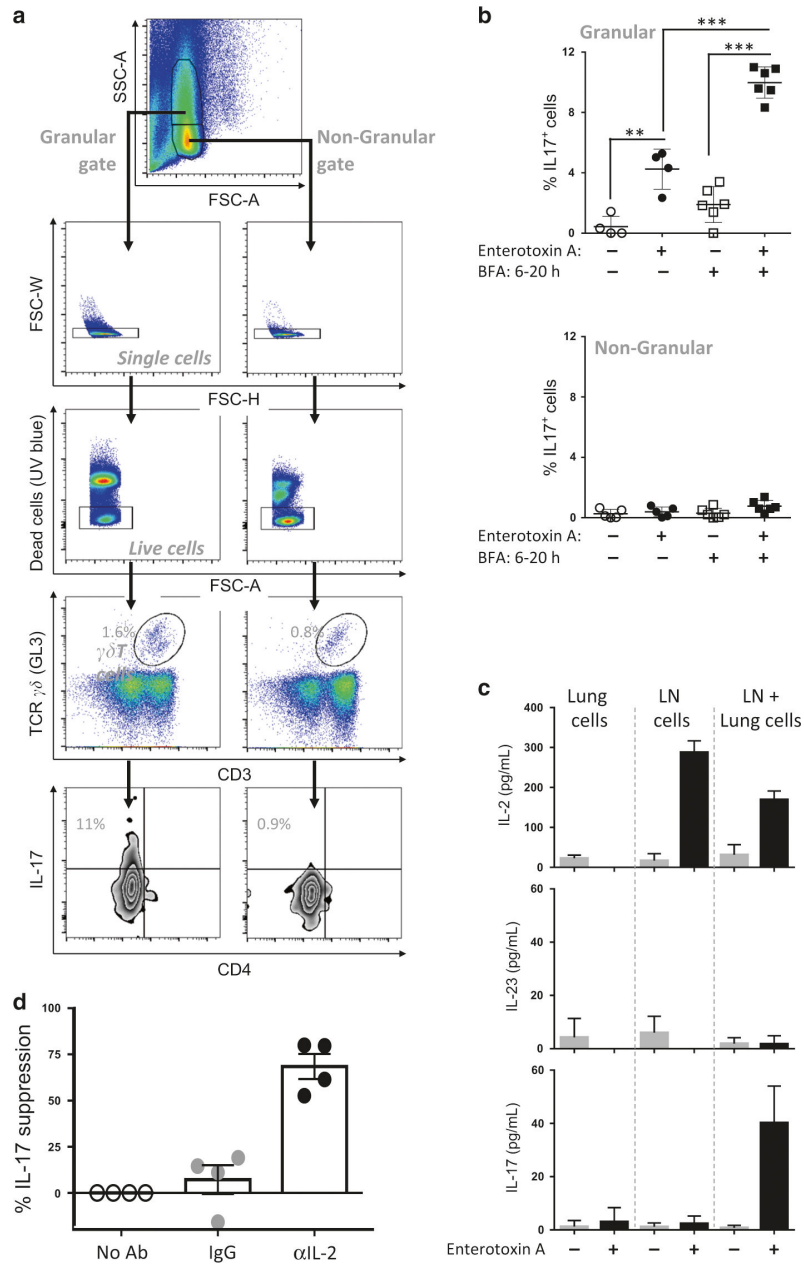
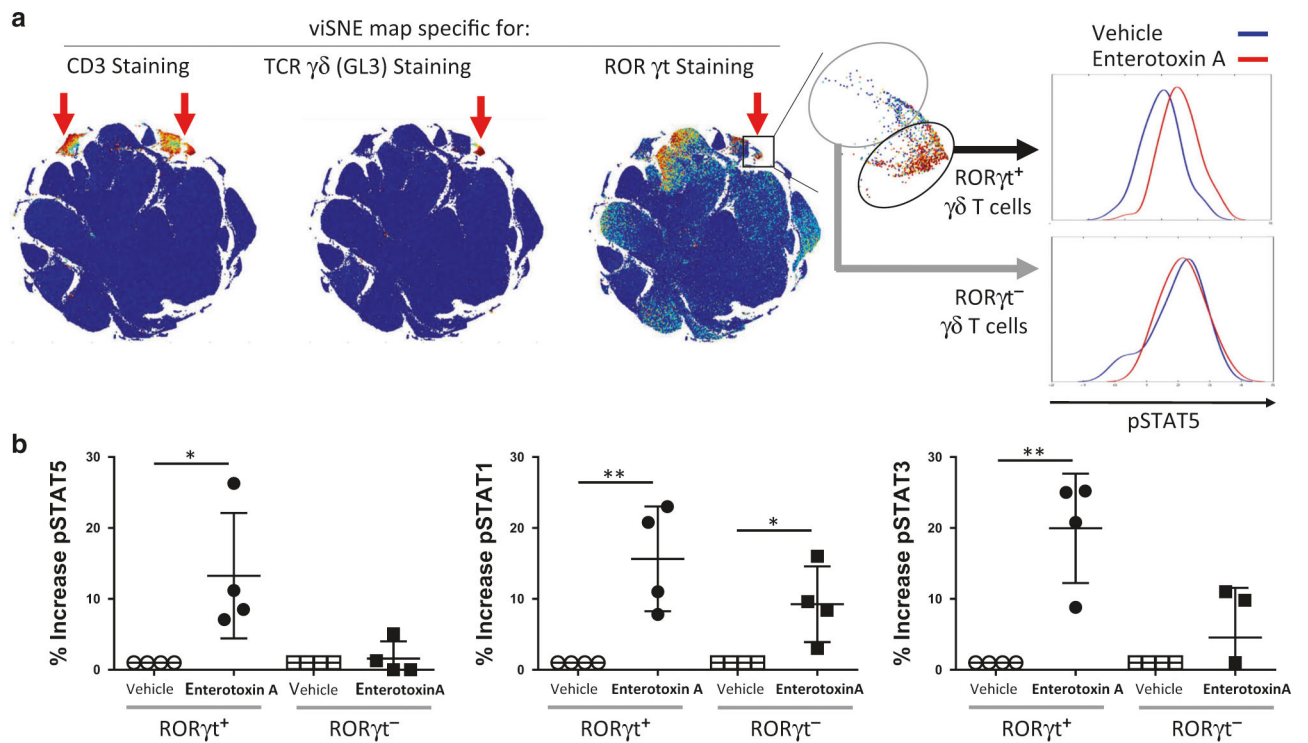
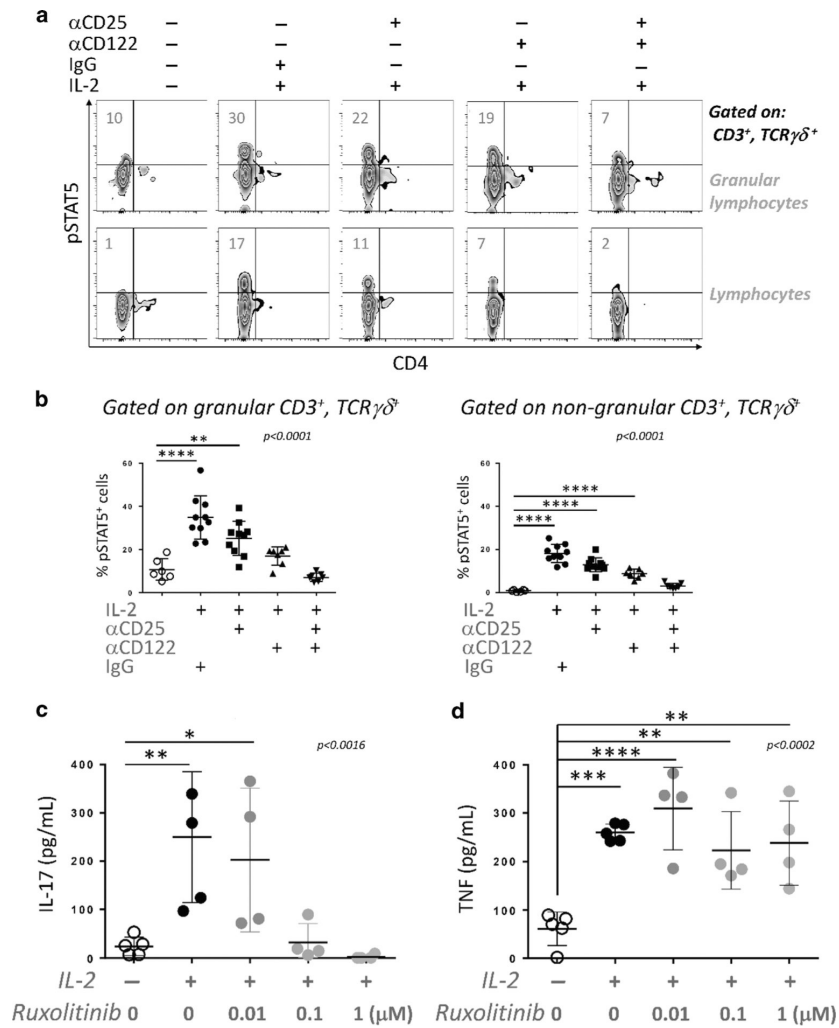


Fig. 1. *S. aureus* enterotoxin A-mediated IL-17 released by Granular $\gamma\delta$ T cells is IL-2 dependent. **a** Lungs cells (2×10^5 /well) and lymph node cells (1×10^5 /well) isolated from naive mice were co-cultured in presence of *S. aureus* enterotoxin A or vehicle for 20 h. At 6 h, BFA was added in the indicated samples. Representative plot and flow cytometry gating strategy are shown. **b** Data were combined from six independent experiments. Each dot represents a biological replicate. Each experiment was performed with pooled lung cells and pooled lymph node cells obtained from 5–10 mice. Data shown are individual biological replicates \pm s.e.m. Statistical significance was evaluated by student's *t*-test. **c** Lung cells and lymph node cells isolated from naive mice were cultured alone and co-cultured (2×10^5 /well) with or without *S. aureus* enterotoxin A. Culture supernatants were obtained after 20 h and

assayed for cytokines by ELISA. One experiment representative of four biological replicate is shown. **d** Lung and lymph node cells co-cultured in the presence of *S. aureus* enterotoxin A with anti-IL-2 blocking antibodies or isotype antibody. Bar graphs show mean \pm s.e.m. Data were combined from four independent experiments. Each experiment was performed with pooled lung cells and pooled lymph node cells obtained from 3–5 mice. Each dot represents an independent biological replicate. Statistical significance was evaluated by two-way ANOVA followed by Sidak's multiple comparisons test

**Fig. 2.**

ROR γt -expressing $\gamma\delta$ T cells phosphorylate STAT5. **a** Lung cells isolated 4 h post i.n. immunization with *S. aureus* enterotoxin A or vehicle were barcoded, pooled, and stained with metal-labeled antibodies and analyzed by mass cytometry (Helios). ViSNE maps were used to identify $\gamma\delta$ T-cell population (CD3⁺ GL3⁺), and ROR γt -expressing cells. Representative histograms of cells expressing pSTAT5 from the gated population are shown for 1 of 4 independent biological replicates. **b** Quantification of the increase of pSTAT5, pSTAT1, and pSTAT3 in ROR γt^+ and ROR γt^- $\gamma\delta$ T-cell populations is shown for four independent experiments, with one *S. aureus* enterotoxin A-treated and one vehicle-treated mouse per experiment. Statistical significance was evaluated by one-way ANOVA followed by Dunnet's test comparing each group to the untreated group

**Fig. 3.**

IL-2 signaling is required for $\gamma\delta$ T cell IL-17 production. **a** Lung cells isolated from naive mice were plated with anti-CD25, anti-CD122, or isotype antibody for 2 h then stimulated with IL-2 or vehicle for 25 min. Cells were fixed, permeabilized, and stained with antibodies specific for CD3, CD4, TCR $\gamma\delta$, and pSTAT5, as well as a live/dead marker. $\gamma\delta$ T cells were gated as in Fig. 1 and the expression of pSTAT5 is presented. One experiment representative of two biological replicates is shown. **b** pSTAT5 expression in $\gamma\delta$ T cells from four combined independent experiments is shown. Data shown are individual biological replicates \pm s.e.m. and each dot represent a mouse. Statistical significance was evaluated by student's *t*-test. **c** Lung cells isolated from naive mice were stimulated with IL-2 or vehicle for 20 h with different doses of Ruxolitinib, a JAK1/2 inhibitor. Culture supernatants were obtained at 15–20 h and assayed for IL-17 by ELISA. **d** In a simultaneous experiment with C, the toxicity of Ruxolitinib was tested. Lung cells were stimulated with a low dose of PMA and ionomycin (P:I) for 20 h with different doses of Ruxolitinib. Culture supernatants were obtained and assayed for TNF by ELISA. IL-17, and TNF production is shown from four combined independent experiments. Each experiment was performed with lung cells obtained from 14–20 mice. Each dot represents an independent biological replicate. Data

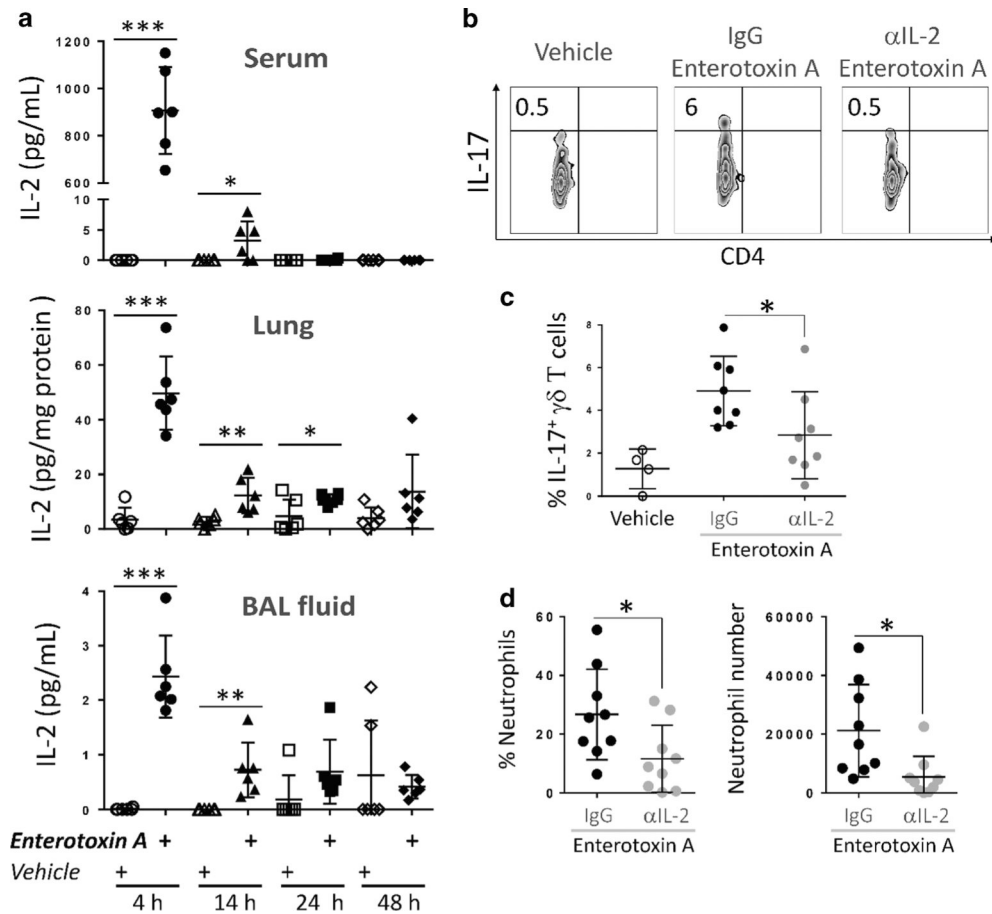
shown are individual biological replicate \pm s.e.m. Statistical significance was evaluated by student's *t*-test

Author Manuscript

Author Manuscript

Author Manuscript

Author Manuscript

**Fig. 4.**

S. aureus enterotoxin A-induced IL-2 contributes to IL-17 production by granular T $\gamma\delta$ 17 cells in vivo. **a** Tissues were harvested at 4, 14, 24, and 48 h after i.n. immunized with *S. aureus* enterotoxin A or vehicle and assayed for IL-2 by ELISA. Data were combined from three independent experiments, $n = 6$ per group. Each dot represent a mouse. Data shown are individual biological replicates \pm s.e.m. **b** Lung cells were purified at 6 h post i.n. *S. aureus* enterotoxin A immunization (0.25 μ g/mouse) from mice pre-treated with IL-2 neutralizing antibody or isotype control. Lung cells were analyzed by flow cytometry as in Fig. 1 and IL-17 expression in granular $\gamma\delta$ T cells is shown. **c** IL-17 expression in granular $\gamma\delta$ T cells (CD3⁺, GL3⁺) from two combined independent experiments is shown. **d** BAL cells were obtained at 8 h after i.n. *S. aureus* enterotoxin A immunization (0.5 μ g/mouse) from mice pre-treated with IL-2 neutralizing antibody or isotype control. BAL cells were analyzed by flow cytometry and neutrophils were identified as CD3⁻, CD19⁻, NK1.1⁻, CD11b⁺, Ly6C⁺, Ly6G⁺ cells. Percentage and total number of neutrophils are shown from two combined independent experiments. Each dot represent a mouse. Data shown are individual biological replicates \pm s.e.m. Statistical significance was evaluated by student's *t*-test

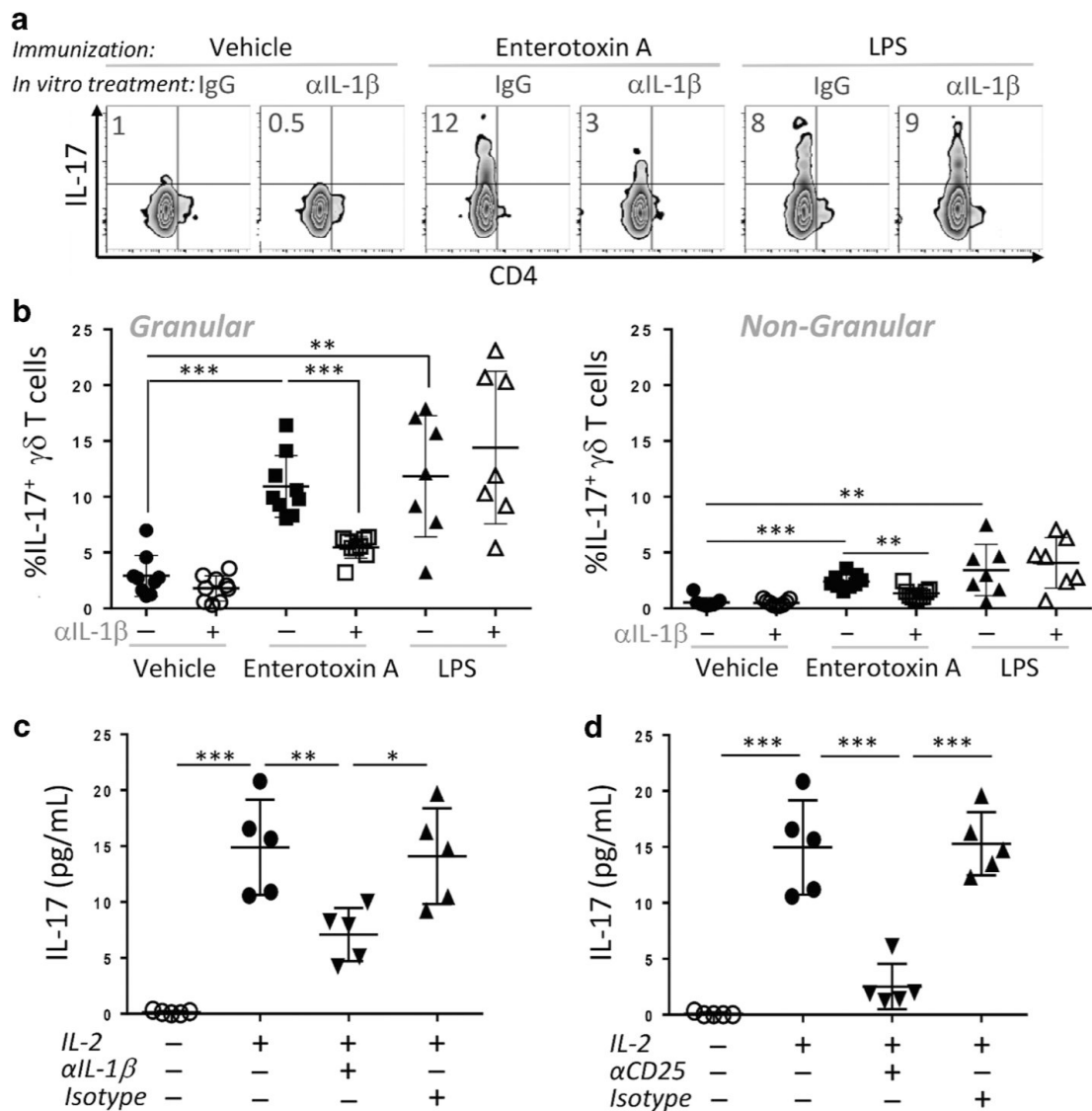


Fig. 5.

IL-1 β contributes to *S. aureus* enterotoxin A-induced IL-17 production by granular $\gamma\delta$ T17 cells in vivo. **a** Lung cells isolated at 6 h post i.n. *S. aureus* enterotoxin A, LPS immunization, or vehicle control were plated for 5 h with anti-IL-1 β neutralizing antibody or isotype control. Cells were analyzed by flow cytometry as in Fig. 1 and IL-17 expression in granular $\gamma\delta$ T cells is shown. **b** IL-17 expression in granular and non-granular $\gamma\delta$ T cells (CD3⁺, GL3⁺) from four combined independent experiments is shown, $n = 7-9$ per group. Each dot represents a mouse. Lung cells isolated from naive mice were stimulated with IL-2 or vehicle for 20 h with **(c)** anti-IL-1 β neutralizing antibody, and in the same experiment with **(d)** anti-CD-25 neutralizing antibody or isotype controls. Culture supernatants were obtained after 20 h and assayed for IL-17 by ELISA. IL-17 production is shown from five combined independent experiments. Each dot represents a biological replicate. Each experiment was performed with pooled lung cells obtained from 10–20 mice. Data shown are individual biological replicates \pm s.e.m

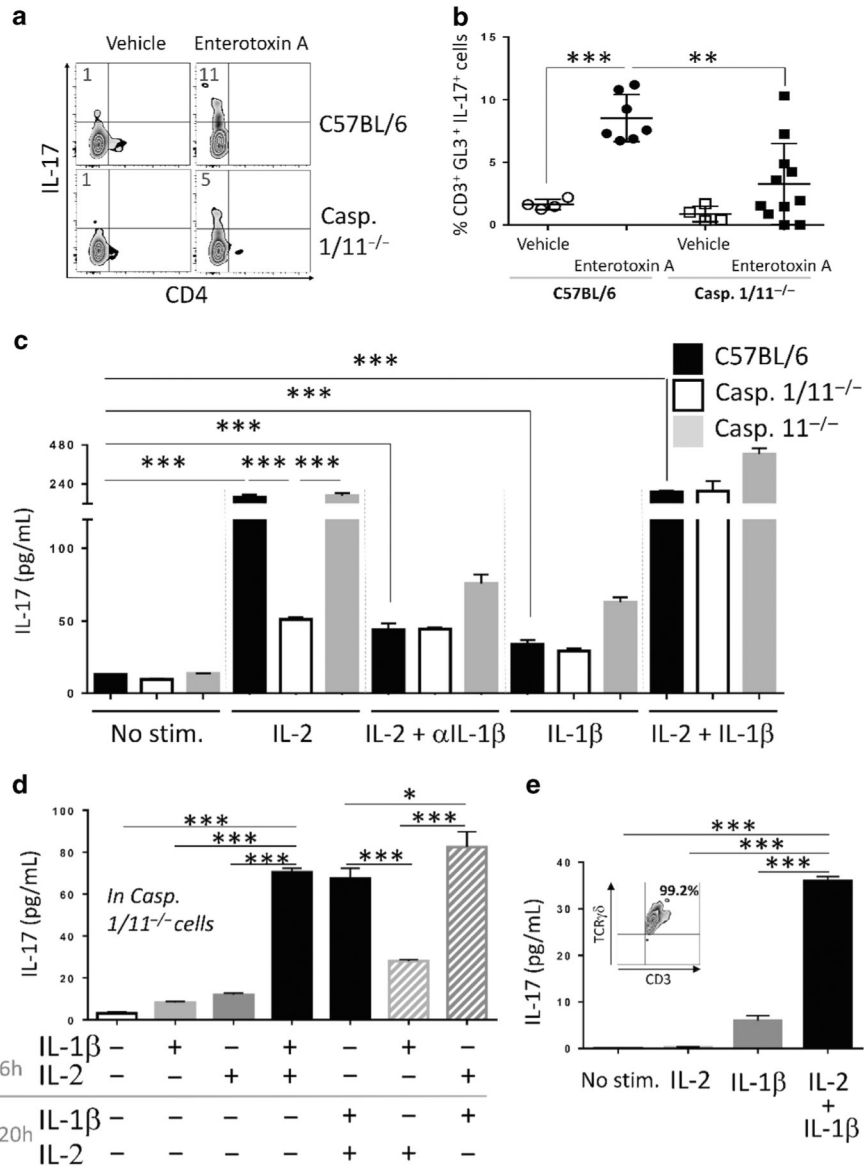


Fig. 6. IL-2 and IL-1β synergize to stimulate IL-17 production. **a** Lung cells were purified 6 h post i.n. *S. aureus* enterotoxin A (1 μg) immunization from wild-type (C57BL/6) and caspase 1/11^{-/-} mice. Lung cells were analyzed by flow cytometry as in Fig. 1 and IL-17 expression in granular γδ T cells is shown. **b** IL-17 expression in granular γδ T (CD3⁺, GL3⁺) cells from four combined independent experiments is shown, *n* = 4–11 per group. Each dot represents a mouse. Data shown are individual biological replicates ± s.e.m. Statistical significance was evaluated by student’s *t*-test. **c** Lung cells isolated from naive wild-type (C57BL/6), caspase 1/11^{-/-}, and caspase 11^{-/-} mice were stimulated with vehicle, IL-2, anti-IL-1β antibody, and IL-1β as indicated. Culture supernatants were obtained after 20 h and assayed for IL-17 and IL-1β by ELISA. Data shown are one experiment representative of three biological replicates. Bar graphs show triplicate ± s.e.m. **d** Lung cells isolated from naive caspase 1/11^{-/-} mice were stimulated with vehicle, IL-1β and IL-2. Cytokines

were added at the indicated time and kept for the entire time of culture. Culture supernatants were obtained after 20 h and assayed for IL-17 by ELISA. Data shown are one experiment representative of three biological replicates. Bar graphs show triplicate \pm s.e.m. Statistical significance was evaluated by student's *t*-test. e Lung $\gamma\delta$ T cells (30,000/well) were purified by flow cytometry and stimulated with vehicle, IL-2 alone, IL-1 β alone, or with IL-2 for 2 h followed by IL-1 β . Culture supernatants were obtained after 20 h and assayed for IL-17. The insert indicates the purity of the sorted $\gamma\delta$ T cells. Data shown are one experiment representative of three biological replicates. Bar graphs show triplicate \pm s.e.m. Statistical significance was evaluated by student's *t*-test